RSC Advances

The Co-adsorption of Cu2+ and Zn2+ with adsorption sites surface-lattice reforming on Calcined Layered Double Hydroxides

Journal:	*RSC Advances*
Manuscript ID:	RA-ART-01-2015-001745.R1
Article Type:	Paper
Date Submitted by the Author:	04-Mar-2015
Complete List of Authors:	Xiao, Yuxin; Shandong University, Environmental science and engineering Sun, Mingming; Shandong University, Environmental science and engineering Su, Jixin; Shandong University, School of Environmental science and engineering Zhang, Lin; Shandong University, Environmental science and engineering Gao, Xue; Shandong University, Environmental science and engineering Zhu, Hong; Shandong University, School of Civil Engineering

The Co-adsorption of Cu^{2+} and Zn^{2+} with adsorption sites surface-lattice reforming on Calcined Layered Double Hydroxides

Yuxin Xiao,[†a] Mingming Sun,[†a] Lin Zhang,[a] Xue Gao, [a] Jixin Su,*[a] Hong Zhu[b]

[a] School of Environmental Science and Engineering, Shandong University, Jinan 250100, China

[b] School of Civil Engineering, Shandong University, Jinan 250100, China

[†]The co-first author

*Phone: +86-531-88362008; fax: +86-531-88362008; E-mail address: jxsu@sdu.edu.cn

ABSRACT: In this paper, the nano-amorphous Mg/Al oxides-calcined layered double hydroxides (CLDHs) was employed to evaluate the adsorption capacity of Cu^{2+}or Zn^{2+} in wastewater and to investigate the adsorption mechanism. The results demonstrated that the maximal adsorption capacities of Cu^{2+} and Zn^{2+} were 422.08 $mg \cdot g^{-1}$ and 508.21 $mg \cdot g^{-1}$, respectively, whereas the initial Cu^{2+}or Zn^{2+} concentration in single-ion solutions was 500 $mg \cdot L^{-1}$. Certain competitive and inhibitory effects were observed during the Cu^{2+} and Zn^{2+} binary ions adsorption. During the process, CLDHs were hydration, and heavy metal ions were adsorbed rapidly onto the surface of CLDHs with crystalline phase inversion and formation of octahedral sheets with positive charges. Then the sheets were stripped into solution and hydroxyls intercalated into the interlayer to make sheets combined together. Consequently CLDHs recovered into hydrotalcite structure, which realized the transition from surface adsorption to bulk phase. Thermodynamics study indicated

that the adsorption isotherm was suitable for Langmuir and kinetic model was the pseudo-second-order. The regenerative adsorption experiments suggested that CLDHs could remove Cu^{2+} or Zn^{2+} with high efficiency with 4 repetitions. Both the high density bulk adsorption sites and the superior performance indicate vast potential application prospect of the material.

Keywords: copper; zinc; magnesium aluminum oxide; competitive adsorption; wastewater purification

1. Introduction

Originally derived from minerals, heavy metals spread unconsciously in the environment, including mining, metal finishing, plating plants, welding and alloy manufacturing, etc.[1]. In the factory, the washing wastewater is deionized water after multistage countercurrent washing. In this experiment, preparing solution by deionized water to simulate the actual wastewater is appropriate. Since heavy metals not only accumulate in the environment and living organisms, but cannot be decomposed as well[2]. In recent years, heavy metal ions in the wastewater significantly threaten the environment and human health. For instance, industrial effluent always contains toxic heavy element, such as zinc, copper, nickel, cadmium and lead, etc., which may gradually accumulate in organisms, thereby resulting in severe diseases or even death [3-5]. Therefore, it is extremely urgent to develop efficient and reliable methods so as to remove metal ions in wastewater. As we all know, substantial methods such as precipitation, coagulation, solvent extraction, electrolysis, membrane

separation, ion exchange and adsorption, have been developed and tested with respect to removal of heavy ions[6, 7]. However, these traditional methods are mainly base on solid surface adsorption and have limited adsorption capability. In addition, from the perspective of life cycling, the metal ions treated with traditional methods are not able to exit the environment in the form of minerals, finally, which was in the stable original mineral state million years ago. Hence, a high-efficient and low-cost method would be ideal for removal of metal ions.

Due to the merits of convenient operation, low cost, potential for regeneration and high retention efficacy, adsorption is believed the most attractive method[8, 9]. In recent years, the nano-adsorbents layered double hydroxides[10] and their calcined products (CLDHs) have attracted widest attention because of the characteristics of large surface area, high density of active surface sites, low intraparticle diffusion resistance and high adsorption capacities. The general formula of LDHs is $[M^{2+}_{1-x} + M^{3+}_{x}(OH)_2]\ [A^{n-}]_{x/n}\cdot yH_2O$, where M^{2+} and M^{3+} are divalent and trivalent metal cations, respectively, such as Mg^{2+} and Al^{3+}, A^{n-} is the incorporated anions in the interlayer space along with water molecules, and x is the ratio of $M^{3+}/(M^{2+}+M^{3+})$[11-13], whereas the adsorption of CLDHs can be expressed as below[14, 15]:

$$Mg_{1-x}Al_xO_{1+x/2} + \frac{x}{n}A^{n-} + (m+1+\frac{x}{2})H_2O + zM^{2+}$$
$$\longrightarrow Mg_{1-x}M_zAl_x(OH)_{(2+2z)}(A^{n-})_{\frac{x}{n}}\cdot mH_2O + (x-2z)OH^-$$

LDHs have high anionic exchange capacity, which allows the limited exchange of their original anions with those present in an aqueous solution. Metal cations in the form of sediments are sorbed on the surface of LDHs. This ability of LDHs can be

used to absorb a variety of anions[11, 16, 17] and metal cations[18-21], which have been researched extensively.

With higher surface area, CLDHs are believed having higher adsorption capacity than the uncalcined ones. CLDHs is a kind of positive charge material on surface with higher isoelectric point [22]. To date, only a few researches discussed the use of CLDHs for heavy metal ions [21, 23] and anions [24] removal and very few of these researches investigated the competitive adsorption of two heavy metal ions, which are ubiquitous in industrial wastewater treatment system. E. Alvarez-Ayuso and Nugteren [23] also confirmed that the removal capacities towards chromium were 16.3 and 128 $mg \cdot g^{-1}$ on uncalcined and calcined LDHs, respectively [23]. CLDHs maybe have a higher removal amount about anions and heavy metal ions than LDHs. Cai Peng and his partner explored competitive adsorption characteristics of fluoride and phosphate on calcined Mg–Al–CO_3 layered double hydroxides (CLDH). They found that the competition in adsorption between fluoride and phosphate was affected by pH, contact time and sequence of addition of the anions.

The objective of this study was to investigate the maximal adsorption capacity, the competitive effect and the regeneration performance of CLDHs for Cu^{2+} and Zn^{2+}. The thermodynamics experiments were designed to explore the maximum adsorption quantity of CLDHs for Cu^{2+} or Zn^{2+} in individual sorption. The adsorption rate and competition effect between Cu^{2+} and Zn^{2+} were obtained by kinetics studies. By successive adsorption/calcinations, the largest circular number of adsorbent (CLDHs) for Cu^{2+} or Zn^{2+} with high removal efficiency could be detected. These results

provided evidence that CLDHs are suitable to be used to treat wastewater containing both Cu^{2+} and Zn^{2+} pollutants. In addition, the mechanism of metal ion removal of CLDHs could be further elucidated based on X-ray diffraction pattern (XRD), X-ray photoelectron spectroscopy (XPS), the Brunauer- Emmett-Teller (BET), scanning electron microscope [25] and electron dispersive X-ray analysis (EDX).

2. Materials and methods

2.1. Chemicals.

The chemicals, $Mg(NO_3)_2 \cdot 6H_2O$, $Al(NO_3)_3 \cdot 9H_2O$, NaOH, Na_2CO_3, $Cu(NO_3)_2 \cdot 3H_2O$ and $Zn(NO_3)_2 \cdot 6H_2O$ were A.R. grade and used as received without purification. All the water used was deionized water. In this study, the stock solutions of copper nitrate (10000 $mg \cdot L^{-1}$) and zinc nitrate solution (10000 $mg \cdot L^{-1}$) were used for synthesized wastewater. An appropriate volume of 0.1M HNO_3 and 0.1M NaOH solution was used to adjust the pH of the solution[26].

2.2. Preparation of $Mg_3Al–CO_3–LDHs$ and CLDHs.

The Mg_3Al-CO_3-LDHs were prepared by the co-precipitation method[27] at a fixed pH 10 ± 0.5, which was as follows: one aqueous solution (400 mL) contained $Mg(NO_3) \cdot 6H_2O$ (0.1875mol) and $Al(NO_3)_3 \cdot 9H_2O$ (0.0625mol, Mg/Al molar ratio 3:1). A second solution (250 mL) contained NaOH (0.4000mol) and Na_2CO_3 (0.0250mol). Then adding them dropwise to high purity water (400mL) under vigorous stirring[28]. The final precipitate was separated by vacuum filtration, and the filter cake was heated at 353K for 24 h to crystallize. Finally Freeze-drying samples and getting $Mg_3Al–CO_3–LDHs$. The calcined production was obtained by heating

LDHs in a muffle furnace at 723 K for 2 h.

2.3. Competitive Adsorption Study.

The solutions were prepared as follows: (1) only Cu^{2+} (100 $mg \cdot L^{-1}$), (2) only Zn^{2+} (100 $mg \cdot L^{-1}$), (3) Cu^{2+} + Zn^{2+} (100$mg \cdot L^{-1}$+100$mg \cdot L^{-1}$) mixture. 50mg CLDHs were mixed with 100 mL of different Cu^{2+}/Zn^{2+} concentrations solutions with a rolling rate of 150 rpm at testing temperature (308.15K)[14]. Besides, the initial pH of them were about 2.1 and adjusted by a certain amount of 0.1M nitric acid solution. Under the time interval 0, 10, 30, 50, 90, 120, 180, 240, 300min, 2mL supernatant were taken to centrifuge, filter respectively and analysis the filtrates by flame atomic absorption spectrophotometer in a TAS-990F instrument[29, 30].

2.4. Adsorption capacity Experiments.

Different concentrations Cu^{2+} or Zn^{2+} solutions (100, 200, 300, 400, 500 $mg \cdot L^{-1}$) were prepared by dilution of the stock solutions, separately. Then the test method was same as before, except for adsorption time, which was set to 5h. And the testing temperature were 298.15K, 308.15K, 323.15K[14].

2.5. Regeneration Adsorption Study.

The possibility of recycling the CLDHs was evaluated by repeating adsorption/calcination experiments. We used 0.3g CLDHs to repeat the adsorb procedures up more than once cycles. The adsorption conditions were as follows: every time, Cu^{2+} (or Zn^{2+}) solution concentration 100$mg \cdot L^{-1}$, reaction temperature 308.15K, pH 2.0 and contact time 5 h [31, 32].

The quantity of Cu^{2+} or Zn^{2+}adsorbed on CLDHs at time t was calculated by the

following equation [33]:

$$q_t = \frac{(C_0 - C_t)V}{W} \quad (2)$$

The removal percentage of Cu^{2+} or Zn^{2+} was calculated using the following equation:

$$\mathrm{Re}\,moval(\%) = \frac{C_0 - C_t}{C_0} \times 100\% \quad (3)$$

where q_t is the quantity of Cu^{2+} or Zn^{2+} adsorbed on CLDHs at the time t ($mg \cdot g^{-1}$), $q_e = q_t$ when adsorption reaches equilibrium, V is the volume of solution(L), C_0($mg \cdot L^{-1}$) and C_t ($mg \cdot L^{-1}$) are the initial concentration of Cu^{2+} or Zn^{2+} and that at time t, W is the mass of adsorbent (g) [34, 35].

2.6. Characterization.

The X-ray diffraction pattern (XRD) analysis used a Rigaku D/MAX-RA instrument at 40 kV and 50 mA with Cu Kα radiation (λ = 0.154184 nm) .The 2θ range from 2° to 70° and the scanning rate was 8ºmin^{-1} [29, 35]. The X-ray photoelectron spectroscopy (XPS) was collected in a Phi 5300 ESCA system (Perkin-Elmer, USA) with Mg Ka (1253.6 eV) radiation (operated at 200 W). The binding energy of C 1s was shifted to 284.6 eV as an internal reference. The specific surface areas were evaluated by the Brunauer-Emmett-Teller (BET) method[36, 37]. Surface area and porosity analysis were using a Quantachrome SI system, which was determined by N_2 adsorption/ desorption at 77 K. The hole distribution of the sample was calculated the BJH model. The surface morphology of the samples were obtained by using a scanning electron microscope (SEM) from a Hitachi S-3000N microscope instrument equipped with the Hitachi electron dispersive X-ray analysis (EDX) microanalysis system.

3. Results and discussion

3.1. Competitive Adsorption.

In order to study the potential mechanism involved in Cu^{2+} and Zn^{2+} sorption for the binary pollutant treatment, three kinetic models were tested: ① the pseudo-first order [15, 38], (2) the pseudo-second order [39], and ③ the particle diffusion kinetic model [40]. The kinetic equations were as follow:

The pseudo-first order: $$\ln(q_e - q_t) = \ln q_e - K_1 t \quad (4)$$

The pseudo-second order: $$\frac{t}{q_t} = \frac{1}{K_2 q_e^2} + \frac{t}{q_e} \quad (5)$$

The particle diffusion: $$q_t = K_i t^{0.5} \quad (6)$$

Where k_1 (min^{-1}), k_2 ($g \cdot mg^{-1} \cdot min^{-1}$) and k_i ($mg \cdot g^{-0.5} \cdot min^{-0.5}$) represent the rate constants of the pseudo-first-order kinetic, pseudo-second-order and particle diffusion model, respectively. The parameters were listed in Table.1. The correlation coefficients (R^2) of pseudo-second-order were the highest among the three models. Moreover, the calculated equilibrium adsorption quantity (q_e) was close to the experimental results for the pseudo-second-order model, indicating the effectiveness of the pseudo-second -order kinetic model in describing the whole process.

The rate constant K_2 for Cu^{2+} adsorption increased from ~3.39×10^{-4} $g \cdot mg^{-1} \cdot min^{-1}$ in the single system to ~3.48×10^{-4} $g \cdot mg^{-1} \cdot min^{-1}$ in the binary system, while the constant for Zn^{2+} adsorption decreased from ~0.64×10^{-4} $g \cdot mg^{-1} \cdot min^{-1}$ to ~0.54×10^{-4} $g \cdot mg^{-1} \cdot min^{-1}$. Thus, the adsorption rate was promoted for Cu^{2+}, but inhibited for Zn^{2+}. Besides, the equilibrium adsorption capacities of Cu^{2+} and Zn^{2+} in single-ion solution were ~140.80 and ~225.95 $mg \cdot g^{-1}$, whereas in binary solutions, the adsorption amount

reduced to ~126.55 and ~213.57 $mg \cdot g^{-1}$, respectively. In this respect, mutual restraint existed between Cu^{2+} and Zn^{2+} in binary adsorption system. For the pseudo-second-order kinetics model, t/q_t curve was fitted as shown in Fig.1. It could be seen that CLDHs removed a considerable amount of Cu^{2+} or Zn^{2+} from the aqueous solutions. The adsorption amounts of Cu^{2+} and Zn^{2+} in the binary system were lower than that in single system, and the inhibition effect was observed with little influence. Therefore, Cu^{2+} and Zn^{2+} could be removed simultaneously from wastewater. Meanwhile, the results also showed that Cu^{2+} and Zn^{2+} competed for the limited number of active sites on CLDHs with equivalent binding force[26]. It can be seen from Fig.1 that the Cu^{2+} uptake was fast for the first 10 min and gradually got closed to saturation after 120 min, while the sorption rate of Zn^{2+} was lower than that of Cu^{2+} within the first 20 min and then continued to increase until 240 min. It took less time for Cu^{2+} to reach adsorption equilibrium than Zn^{2+}, which reflected that not only was the adsorption rate of Cu^{2+} faster than that of Zn^{2+}, but Cu^{2+} was easier to reach adsorption equilibrium as well. It terms of the adsorption amount, CLDHs showed better adsorption ability for Zn^{2+} [41, 42].

3.2. Adsorption capacity.

To investigate the removal capacity of CLDHs for Cu^{2+} and Zn^{2+}, two common adsorption isotherm models, namely Langmuir isotherm [28] and Freundlich isotherm[37] were selected. The corresponding isotherm equations are expressed as follows:

Langmuir: $$\frac{C_e}{q_e} = \frac{1}{q_{\max} K_L} + \frac{C_e}{q_{\max}} \quad (7)$$

Freundlich: $\ln q_e = \ln K_F + \frac{1}{n}\ln C_e$ (8)

where C_e ($mg \cdot L^{-1}$) is the concentration of the ions adsorption equilibrium; q_{max} (mg/g) is the maximum adsorption amount; K_L(1/mg) and $K_F(mg \cdot g^{-1}) \cdot (L \cdot mg^{-1})^{1/n}$ are Langmuir and Freundlich constant, respectively[14, 39, 43].

The parameters of Langmuir and Freundlich isotherms were calculated and compared, as shown in Table.2. It can be seen that the Langmuir equation better fits the adsorption isotherms with R^2 over 0.99, suggesting that the adsorption process was homogeneous with multitudinous active sites. The adsorption isotherms of CLDHs for Cu^{2+} and Zn^{2+} at various temperatures were shown in Fig.2. It could be seen that the adsorption isotherms experienced similar patterns for Cu^{2+} and Zn^{2+}. The removal amounts were linearly proportional to the concentrations of the metal equilibrium and the reaction temperatures [19]. While the concentrations of metal equilibrium increased with increasing initial concentration. So, in this experiment, the adsorption capacities of CLDHs for Cu^{2+} and Zn^{2+} were maximum with initial Cu^{2+}or Zn^{2+} concentration of 500mgL^{-1}, and reaction time of 300 minutes under 323.15K.

3.3. Regenerative Adsorption.

It is of great economic value to evaluate the regenerative behavior of the adsorbents. In order to study the recycling of CLDHs as adsorbents for Cu^{2+} and Zn^{2+}, the thermal regeneration tests were carried out. In the experiment, the removal efficiency of Cu^{2+} and Zn^{2+} with respect to each cycle was shown in Fig.3. It can be seen that all Cu^{2+} and Zn^{2+}could be almost removed after four adsorption processes. The removal efficiency of Cu^{2+} and Zn^{2+} declined to 44.41% and 78.06% in the fifth cycle. The

experiment suggested that the thermal regeneration of CLDHs was acceptable within four cycles. CLDHs can take advantage of the anions and metal cations in solution to regenerate the Hydrotalcite-like compounds. The results might be caused by a certain amount of CLDHs tending to adsorption equilibrium. The CLDHs successively proceeded adsorption/calcination and progressively led to decreased crystallinity of new products[44, 45]. With limited active sites, the adsorption process gradually tended to balance as the cycling time increased. It was obtained that the overall amount of adsorption of Cu^{2+} and Zn^{2+} on CLDHs reached 283.901 $mg \cdot g^{-1}$ and 306.746 $mg \cdot g^{-1}$, respectively, after adsorption of five times [37]. Compared with relevant literatures[4, 6]. CLDHs demonstrated stronger regeneration performance and higher practical application value. Adsorption products belong to one kind of clays, which is closed to the original source of metal and met the requirement of life cycle.

3.4. Sample Characterization.

The X-ray diffraction (XRD) patterns of precursor Mg_3Al-CO_3-LDH, and CLDHs pre- and post-adsorption of Cu^{2+} and Zn^{2+} were shown in Fig.4. For LDHs, sharp and symmetric peaks for (003) and (006), which were the characteristic of hydrotalcite-like compounds could be seen, indicating that the material consisted of a single crystalline phase. For CLDHs, because calcining destroyed the layered octahedral structure of crystal LDHs, the interlayer water and anions disappeared. The internal structure of CLDHs become chaotic, which were composed of mixed oxide Mg(Al)O. Therefore, in Fig.4 (a), the peaks of CLDHs were completely missing and only two different peaks (200) and (220) were exhibited[12,46,47]. The peaks of

CLDHs-Cu and CLDHs-Zn were similar to that of LDHs. CLDHs gradually reconstructed the structure of the hydrotalcite-like compounds while adsorbing Cu^{2+} and Zn^{2+}. Besides, the peaks of copper hydroxide and zinc hydroxide could not be found, suggesting that Cu^{2+} or Zn^{2+} also participated in the refactoring process and were not be adsorbed on the surface of CLDHs in a form of precipitation, finally. The elements isomorphous substitution effect in crystalline materials typically resulted in variations of XRD patterns[19]. Compared with LDHs patterns, the relative intensities of peaks of CLDHs-Cu and CLDHs-Zn decreased, and the abscissas of peaks were of certain deviation. Thus, XRD patterns of Mg/Al-LDH were affected by substitution of Mg^{2+} with Cu^{2+} or Zn^{2+} because of the difference in ion size[10]. The changes of crystal lattice parameters could further proved the isomorphous substitution effect.

To study the adsorption mechanism and sites of Cu^{2+} and Zn^{2+} on CLDHs, the XPS spectra of the CLDHs before and after Cu^{2+} and Zn^{2+} sorption were analyzed. The XPS spectra of the pristine CLDHs and CLDHs-Cu and Zn samples were displayed in Fig.5. Comparing with the pristine CLDHs, new peaks at binding energy of 933.7 eV and 1021.9 eV, attributed to Cu 2p and Zn 2p, were observed in XPS spectrum of CLDHs-Cu and Zn, indicating that Cu and Zn anions are adsorbed on CLDHs. The high-resolution XPS (HR-XPS) is used to investigate elemental composition and oxidation states on the surface. The HR-XPS spectra of CLDHs-Cu-1 (adsorption of one cycle) and CLDHs-Cu-2 (adsorption of five cycles until saturated) were shown in Fig.6 (a) and (b) and CLDHs-Zn-1 and CLDHs-Zn-2 in Fig.7 (a) and (b). The dominant peak appeared at 933.6 eV is ascribed to Cu $2p_{3/2}$ in

Fig.6 (a) (b) and the Zn $2p_{3/2}$ peak appeared at 1021.7 eV which is shown in Fig.7 (a) and (b). From Fig.5, there are four elements C, O, Mg and Al on the surface of CLDHs. In Fig.6 (a), the XPS-peak-differentation-imitating result shows that a peak is 932.1 eV and the other one is 934.6 eV, which illustrates there are two kinds of state of copper ions on the surface of CLDHs adsorption Cu^{2+} at one cycle. The peak at 934.5Ev is attributed to Cu-O-Al and Cu-O-Mg is on the peak position of 932.1eV. It means that copper, magnesium, aluminum and hydroxyl combine on the surface of adsorbent, forming lamellar structure of co-sided octahedron. Discovered through comparative analysis and combined with copper binding energy data tables, a new peak is observed in Fig.6 (b) which is attributed to $Cu(OH)_2$. It also indicates that the whole adsorption sites of CLDHs are occupied after adsorption saturation and the redundant Cu^{2+} only accumulate on the surface of the adsorbent by the formation of Cu-O-Cu. Fig.7 shows the high resolution of XPS spectrum of Zn^{2+}, which can obtain the same result as Cu^{2+}. In Fig.7(a), one peak at 1021.7eV is Zn-O-Al, another 1021.0eV is Zn-O-Mg. A new peak 1022.8eV, displayed in Fig.7, is ascribed to $Zn(OH)_2$. It shows from the result that before adsorption saturation, Cu-O-Cu and Zn-O-Zn do not appear on the surface of CLHDs. Cu^{2+} and Zn^{2+} are bound with magnesium and aluminum to insert onto the laminate, without self-aggregation phenomenon, which shows the uniformity and richness of adsorption sites. The conclusion is consistent with the regeneration experiment, XRD and EDX.

The crystal cell parameters a and c were calculated from (110) and (003) reflections, respectively, which were a=2·d110 and c=3·d003. The basal spacing (d003)

is about 0.770nm and the basal spacing (d110) is about 0.150nm. The interlayer spacing of LDH, CLDHs-Cu and CLDHs-Zn, were list in Table.3. It can be seen that "a" slightly changed, which indicated that the layer thickness was almost constant. The size of parameter "a" was only related to the bond length of M-O (M represents metal elements) and the charges of metal ions. Given the fact that Cu^{2+}, Zn^{2+} and Mg^{2+} have the same charge, and insignificantly different bond lengths, the parameter "a" of LDH, CLDHs-Cu and CLDHs-Zn were close. On the other hand, the parameter "c" not only related to M-O bond length and the charges of the metal ions, but also depended on the interlayer anionic radius and the size of electrostatic interactions of interlayer anionic with positively charged sheets. So the layer board structure of CLDHs-Cu and CLDHs-Zn become distorted compared to that of LDHs. For CLDHs-Cu and CLDHs-Zn, OH^- was the main interlayer anions. Therefore, the parameter "c" and interlayer spacing of CLDHs-Cu and CLDHs-Zn were all bigger than that of LDHs. As a result, the variations of crystal lattice parameters further proved the isomorphous substitution of Cu^{2+} or Zn^{2+} for Mg^{2+}. Cu^{2+} or Zn^{2+} was removed in the form of product composition, rather than Cu or Zn hydroxyl.

The N_2 adsorption and desorption isotherms and pore size distribution of the LDHs and CLDHs were shown in Fig.8. The N_2 adsorption and desorption isotherms were followed the type IV adsorption isotherms according to the IUPAC classification with a H_3-type hysteresis loop for the desorption isotherm, which was the characteristic type of mesoporous materials [48]. At high p/p_0 values, the adsorption

isotherm did not have a plateau, which indicated that N_2 physico-sorption occurred between the aggregates of platelets particles, accounting for the lamellar morphology of the samples. The surface area and pore size distribution were determined with BJH method, which could be seen that the pore distribution of CLDHs was more abundant than LDH in the 3 to 20nm range. The inference was layer boards collapse and molecular dehydration contraction after calcination. A similar situation also appeared in the range of 20 to 50 nm. Mesoporous was the main contribution of the pore volume and specific surface area for LDHs and CLDHs. Therefore, the samples were mesoporous materials[49, 50]. The experimental data were list in Table.4. The surface area of CLDHs was 260.700 $m^2 \cdot g^{-1}$, which was evidently larger than that of LDH (79.727$m^2 \cdot g^{-1}$). Thus, CLDHs could offer much more active adsorption sites, and consequently had higher metal adsorption capacity.

In order to speculated the adsorption mechanism of CLDHs for Cu^{2+} or Zn^{2+} and obtain more information concerning the alteration of the surface morphology, the scanning electron microscopy (SEM) images and corresponding electron dispersive X-ray (EDX) were performed. Fig.9 displayed the high vacuum SEM images of gold-coated LDHs, CLDHs, CLDHs-Cu and CLDHs-Zn with 1 μ m in length and 100-200nm thickness. The alveolate-like structure of LDHs could be clearly seen in Fig.9(a), which was the typical particle morphology of hydrotalcite - like compounds. Fig.9(b) demonstrated that the structures of CLDHs were compact, because that LDHs layer sheets structure collapsed and molecular contracted after calcination. Then the hydrotalcite -like structures disappeared. It also confirmed the pore size distribution

329 results obtained from Fig.8. As seen in Fig.9(c) and (d), the CLDHs-Cu and
330 CLDHs-Zn showed the alveolate-like structures of hydrotalcite-like compounds.
331 Basically, CLDHs retained the structure of LDHs after adsorbing Cu^{2+} or Zn^{2+}.
332 During conversion of CLDH to LDH, the effect of Cu^{2+} or Zn^{2+} was not significant.
333 The EDX images analyzed the relative content of CLDHs components before and
334 after Cu^{2+} and Zn^{2+} adsorption. It can be seen from the Fig.9 that the EDX spectrum
335 of CLDHs mainly contained three components: i.e. oxygen, magnesium, aluminum
336 and carbon, which confirmed that CLDHs were mainly composed of magnesium
337 oxide and aluminum oxide. In the EDX spectrum images of CLDHs-Cu and
338 CLDHs-Zn, the element spectra of copper, zinc and carbon could be also found.
339 Compared with the CLDHs, Cu^{2+}, Zn^{2+} and carbonate intercalated the structure of
340 CLDHs-Cu and CLDHs-Zn. It can be concluded from the above SEM and EDX that
341 Cu^{2+} or Zn^{2+} participated in the structure restructuring of hydrotalcite-like compounds.

342 **3.5. Potential Adsorption Mechanism of CLDHs for Cu^{2+} or Zn^{2+}.**

343 The above adsorption experiments showed that the CLDHs were cost-effective and
344 convenient for removing Cu^{2+} or Zn^{2+} from aqueous solution. Meanwhile, it also
345 demonstrated that Cu^{2+} or Zn^{2+} firstly generated hydroxide precipitation and occurred
346 to metastasis of the water - solid phase. Based on the characterization results of XRD,
347 XPS, SEM and EDX, CLDHs could recover the structure of hydrotalcite-like
348 compounds after adsorbing Cu^{2+} or Zn^{2+}. In the adsorption process, copper or zinc
349 integrated in the sheets. Considering the adsorption mechanism, there were some

inferences: (1) when the particles of Mg/Al-CLDHs contacted the aqueous solution, hydrolysis of mixed oxides occurred in the surfaces and metal hydroxides were formed. Meanwhile, due to the effect of ionization, a certain amount of hydroxyl was released into the solution, contributing to increased pH value. (2) Cu^{2+} or Zn^{2+} in the wastewater would combine with hydroxyl, thereby forming metal hydroxides, most of which were attached to the surfaces of CLDHs because of the high OH^- solution gradient. In addition, copper hydroxide prevailed over zinc hydroxide at the beginning of the reaction, which was probably resulted from the relative stability of copper hydroxide (Ksp= 2.2×10^{-20}) to zinc hydroxide (Ksp= 1.2×10^{-17}). (3) With the ionization effect of metal hydroxides, Mg^{2+}, Al^{3+} and Cu^{2+} (Zn^{2+}) were released again from the interface of the water and CLDHs. With continuous accumulation, the magnesium, aluminum, copper, zinc and hydroxyls combined together on the surface of adsorbents, thus the single octahedral sheet with sharing edges were formed. The Mg^{2+} could be isomorphous substitution with Cu^{2+} or Zn^{2+} because of the same charge, which could transfer a large number of Cu^{2+} or Zn^{2+} from water phase to solid phase, and remove them from wastewater. (4)The sheets were stripped from the sorbent surface to water, which could not combine together, because that the existence of trivalent cations Al^{3+} resulted in electropositive sheets. (5)The above reactions (4 steps) proceeded on the new surface of the adsorbent in oxide state, so a mass of heavy metal ions were removed from liquid phase, producing more single-sheet octahedral groups with positive charges. To balance the charge and keep stable structure, the negative ions (OH^-) were inserted into the interlayer galleries upon

electrostatic interaction. Some water molecules and nitrate anions also automatically inserted into the interlayers. (6) Through constantly cycling of the above reactions, the main layers structures of hydrotalcite -like compounds were reshaped[51]. The adsorption process transformed CLDH to hydrotalcite-like compounds. The regenerative adsorption experiments implemented successional adsorption/calcinations and the adsorption mechanism as described above. Herein, CLDHs have high adsorption capacity and performance of regeneration. The adsorption mechanism for Cu^{2+} and Zn^{2+} were similar, so taking Cu^{2+} as an example, the adsorption process could be expressed as follows:

$$Sur_1\text{-}O\text{-} + H_2O \longrightarrow Sur_1\text{-}O\text{-}...H + OH^- \quad (9)$$

$$Sur_1\text{-}O\text{-} + Cu^{2+} + OH^- \longrightarrow Sur_1\text{-}O\text{-}...Cu(OH) \quad (10)$$

$$Sur_1\text{-}O\text{-}...Cu(OH) \longrightarrow Sur_2(\text{include -Cu-})\text{-}OH \quad (11)$$

Regenerative adsorption process was continued as follows:

$$Sur_2(\text{include -Cu-})\text{-}OH \xrightarrow[\triangle]{723K} Sur_3\text{-}O\text{-} + H_2O \quad (12)$$

$$Sur_3\text{-}O\text{-} + H_2O \longrightarrow Sur_3\text{-}O...H + OH^- \quad (13)$$

$$Sur_3\text{-}O\text{-} + Cu^{2+} + OH^- \longrightarrow Sur_3\text{-}O...Cu(OH) \quad (14)$$

$$Sur_3\text{-}O...Cu(OH) \longrightarrow Sur_4(\text{include -Cu-})\text{-}OH \quad (15)$$

.. ...

Where Sur and Sur_n (n=1, 2, 3.....) respects the structures of the hydrotalcite-like compounds excepting for the hydroxyl groups on the surface.

Conclusions

In this study, a potential CLDHs material was compounded by co-precipitation

method and used to adsorb Cu^{2+} and Zn^{2+} from single and binary systems. According to the experimental results, when the initial Cu^{2+}or Zn^{2+} concentration in single-ion solutions was 500 $mg \cdot L^{-1}$ with the adsorbent dosage of 0.5$g \cdot L^{-1}$, the maximal adsorption capacities of Cu^{2+} and Zn^{2+} were 422.08 $mg \cdot g^{-1}$ and 508.21 $mg \cdot g^{-1}$, indicating that this material may be an effective adsorbent. The results of co-adsorption on CLDHs show that when Cu^{2+} and Zn^{2+} coexist in the water, the adsorption amount is still very large despite the competition between them, which is of great significance for using CLDHs to remove the various toxic heavy ions in wastewater, simultaneously. Through regenerative experiments it was concluded that the CLDHs kept high adsorption efficiency within 4 cycles.

Characterization results show the adsorption of Cu^{2+} and Zn^{2+} on CLDHs layer board is homogeneous. Due to the hydration and ionization on the CLDHs surface, hydroxyls were released to combine heavy metal ions, forming hydroxides (single octahedral sheets with sharing edges) with positive charges, which were stripped from the sorbent surface. The anions entered the interlayer space along with H_2O, which made sheets combined to recover into hydrotalcite structure. And the adsorption was a process that surface adsorption phase shifted to bulk phase, rather than only was the traditional interface adsorption. The equilibrium adsorption data of Cu^{2+} and Zn^{2+} fitted well with the Langmuir model and the adsorption kinetics followed a pseudo-second order model.

Acknowledgments

This work was supported by Science and Technology Development Plan of

Shandong Province (No.2012GGE27098), which is gratefully acknowledged.

REFERENCES

1. F. Ge, M. M. Li, H. Ye and B. X. Zhao, *J. Hazard. Mater.*, 2012, **211-212**, 366-372.
2. T. Wang, Z. Cheng, B. Wang and W. Ma, *Chem. Eng. J.*, 2012, **181-182**, 182-188.
3. R. Rojas, M. R. Perez, E. M. Erro, P. I. Ortiz, M. A. Ulibarri and C. E. Giacomelli, *J. Colloid Interface Sci*, 2009, **331**, 425-431.
4. S. Veli and B. Alyuz, *J. Hazard. Mater*, 2007, **149**, 226-233.
5. L. Zhang, X. W. Su, Z. X. Zhang, S. M. Liu, Y. X. Xiao, M. M. Sun and J. X. Su, *Enviro. Sci. Pollut. Res.*, 2014, **10**, 100-108.
6. J. Gong, T. Liu, X. Wang, X. Hu and L. Zhang, *Environ. Sci. Technol.*, 2011, **45**, 6181-6187.
7. Q. Chen, Z. Luo, C. Hills, G. Xue and M. Tyrer, *Water Res.*, 2009, **43**, 2605-2614.
8. G. Crini, *Prog. Polym. Sci.*, 2005, **30**, 38-70.
9. J. Saiz, E. Bringas and I. Ortiz, *J. Chem. Technol. Biotechnol.*, 2014, **89**, 909-918.
10. Y. Lin, Q. Fang and B. Chen, *J. Environ. Sci.*, 2014, **26**, 493-501.
11. Y. Li, Z. Shahrivari, K.T. P. Liu, M. Sahimi and T. T. Tsotsis, *Ind. Eng. Chem. Res.*, 2005, **44**, 6804-6815.
12. I. Pavlovic, C. Barriga, M. C. Hermosín, J. Cornejo and M. A. Ulibarri, *Appl. Clay. Sci.*, 2005, **30**, 125-133.
13. I. M. Ahmed and M. S. Gasser, *Appl. Surf. Sci.*, 2012, **259**, 650-656.
14. L. Lv, J. He, M. Wei, D. G. Evans and X. Duan, *Water Res.*, 2006, **40**, 735-743.
15. N. K. Lazaridis and D. D. Asouhidou, *Water Res.*, 2003, **37**, 2875-2882.
16. M. Dadwhal, M. Sahimi and T. T. Tsotsis, *Ind. Eng. Chem. Res.*, 2011, **50**, 2220-2226.
17. K. H. Goh, T. T. Lim and Z. Dong, *Water Res.*, 2008, **42**, 1343-1368.
18. R. Bushra, M. Shahadat, A. S. Raeisssi and S. A. Nabi, *Desalination*, 2012, **289**, 1-11.
19. M. Park, C. L. Choi, Y. J. Seo, S. K. Yeo, J. Choi, S. Komarneni and J. H. Lee, *Appl. Clay. Sci.*, 2007, **37**, 143-148.
20. M. R. Pérez, I. Pavlovic, C. Barriga, J. Cornejo, M. C. Hermosín and M. A. Ulibarri, *Appl. Clay. Sci.*, 2006, **32**, 245-251.
21. X. Yuan, Y. Wang, J. Wang, C. Zhou, Q. Tang and X. Rao, *Chem. Eng. J.*, 2013, **221**, 204-213.
22. X. X. Dongxiang Li, Jie Xu, Wanguo Hou, *Colloids and Surfaces A: Physicochemical and Engineering Aspects*, 2011, **348**, 585– 591.
23. E. Alvarez-Ayuso, H. W. Nugteren, *Water Res.*, 2005, **39**, 2535-2542.
24. D. Wan, H. Liu, R. Liu, J. Qu, S. Li and J. Zhang, *Chem. Eng. J.*, 2012,

195-196, 241-247.
25. T. S. Anirudhan, S. Jalajamony, and S. S. Sreekumari, *J. Chem. Eng. Data.*, 2013, **58**, 24-31.
26. H. Zaghouane-Boudiaf, M. Boutahala and L. Arab, *Chem. Eng. J.*, 2012, **187**, 142-149.
27. Q. Z. Yang, Y. Y. Chang and H. Z. Zhao, *Water Res.*, 2013, **47**, 6712-6718.
28. K. Yang, L. G. Yan, Y. M. Yang, S. J. Yu, R. R. Shan, H.Q. Yu, B.C. Zhu and B. Du, *Sep. Purif. Technol.*, 2014, **124**, 36-42.
29. Y. Li, B. Gao, T. Wu, W. Chen, X. Li and B. Wang, *Colloids Surf., A-Physicochem. Eng. Asp.,* 2008, **325**, 38-43.
30. V. C. Srivastava, I. D. Mall and I. M. Mishra, *Colloids Surf., A-Physicochem. Eng. Asp.*, 2008, **312**, 172-184.
31. Y. Li, , H. Y. Bi and Y. B. Zang, *Sep. Purif. Technol.*, 2013, **116**, 448-453.
32. D. S. Tong, M. Liu, L. Li, C. X. Lin, W. H. Yu, Z. P. Xu and C. H. Zhou, *Appl. Clay. Sci.*, 2012, **70**, 1-7.
33. G. X. Yang and H. Jiang, *Water Res.*, 2014, **48**, 396-405.
34. K. S. Triantafyllidis, E. N. Peleka, V. G. Komvokis and P. P. Mavros, *J. Colloid Interface Sci.,* 2010, **342**, 427-436.
35. Y. J. Li, M. Yang, X. J. Zhang, T. Wu, N. Cao, N. Wei, Y. J. Bi and J. Wang, *J. Environ. Sci.*, 2006, **18**, 23-28.
36. Y. X. Zhang, X. D. Hao, M. Kuang, H. Zhao and Z. Q. Wen, *Appl. Surf. Sci.*, 2013, **283**, 505-512.
37. D. Chen, Y. Li, J. Zhang, W. Li, J. Zhou, L. Shao and G. Qian, *J. Hazard. Mater.*, 2012, **243**, 152-160.
38. L. Hakanson, A. C. Bryhn and J. K. Hytteborn, *Sci. Total Environ.*, 2007, **379**, 89-108.
39. Y. S. Ho, G. McKay, *Water. Res.*, 2000, **34**, 723-742.
40. M. Jansson-Charrier, E. Guibal and J. Roussy, *Water. Res.*, 1996, **30**, 465-475.
41. Z. M. Ni, S. J. Xia, L. G. Wang, F. F. Xing and G. X. Pan, *J. Colloid Interface Sci.*, 2007, **316**, 284-291.
42. T. Kameda, T. Yoshioka, T. Mitsuhashi, M. Uchida and A. Okuwaki, *Water Res.*, 2003, **37**, 4045–4050.
43. Y. S. Ho and G. McKay, *Process. Saf. Environ.*, 1999, **77**, 165-173.
44. M. Dakiky, M. Khamis, A. Manassra and M. Mer'eb, *Adv. Environ. Res.*, 2002, **6**, 533–540.
45. P. Cai, H. Zheng, C. Wang, H. Ma, J. Hu, Y. Pu and P. Liang, *J. Hazard. Mater.*, 2012, **213-214**, 100-108.
46. D. Wan, H. Liu, R. Liu, J. Qu, S. Li and J. Zhang, *Chem. Eng. J.*, 2012, **195-196**, 241-247.
47. O. D. Pavel, R. Bîrjega, M. Che, G. Costentin, E. Angelescu and S. Şerban, *Catal. Commun.*, 2008, **9**, 1974-1978.
48. N. Das and R. Das, *Appl. Clay. Sci.*, 2008, **42**, 90-94.
49. G. Wu, X. Wang, B. Chen, J. Li, N. Zhao, W. Wei and Y. Sun, *Appl. Catal., A:*

General, 2007, **329**, 106-111.
50. Y. Guo, Z. Zhu, Y. Qiu and J. Zhao, *J. Hazard. Mater.*, 2012, **239-240**, 279-288.
51. Y. M. Yang, X. F. Zhao, Y. Zhu and F. Z. Zhang, *Chem. Mater.*, 2012, **24**, 81-87.

Table:

Table.1. Kinetic parameters of pseudo-first-order, pseudo-second-order and intraparticle diffusion models at test temperature (308.15K) for Cu^{2+} and Zn^{2+} in single/binary system.

		Pseudo-first-order			**Pseudo-second-order**			**Particle diffusion**	
	$q_{e,exp}$ (mg·g^{-1})	$q_{e,cal}$ (mg·g^{-1})	K_1 (min^{-1})	R^2	$q_{e,cal}$ (mg·g^{-1})	K_2(×10^{-4}) (g·mg^{-1}·min^{-1})	R^2	K_{int} (mg·g$^{-0.5}$·min$^{-0.5}$)	R^2
				Single	**System**				
Cu(II)	140.80	90.70	0.0139	0.9598	148.59	3.39	0.9992	7.31	0.8182
Zn(II)	225.95	192.77	0.0099	0.9865	263.16	0.64	0.9956	13.17	0.9678
				Binary	**System**				
Cu(II)	126.55	84.85	0.0142	0.9705	134.23	3.48	0.9983	6.56	0.8286
Zn(II)	205.59	185.08	0.0095	0.9813	257.73	0.54	0.9959	6.40	0.8286

Table.2**.** Isotherm parameters obtained by using linear method for the adsorption of Cu^{2+} and Zn^{2+}on LDH at different temperatures.

		Langmuir adsorption model			**Freundlich adsorption model**		
	T (K)	**Q_{max} ($mg \cdot g^{-1}$)**	**K_L ($L \cdot mg^{-1}$)**	**R^2**	**K ($(mg \cdot g^{-1}) \cdot (L \cdot mg^{-1})^{1/n}$)**	**n**	**R^2**
Cu(Ⅱ)	298.15	571.43	0.0046	0.9989	9.9353	1.61	0.9885
	308.15	662.25	0.0043	0.9919	10.3034	1.57	0.9959
	323.15	775.19	0.0040	0.9992	9.3416	1.47	0.9906
Zn(Ⅱ)	298.15	434.78	0.0199	0.9979	75.1450	3.12	0.9828
	308.15	476.19	0.0226	0.9920	72.7244	3.20	0.9895
	323.15	584.80	0.0217	0.9914	70.7082	2.78	0.9902

Table.3. The cell parameter a, c and interlayer spacing of LDH, CLDH-Cu and CLDH-Zn.

Parameters	Samples		
	LDH	CLDH-Cu	CLDH-Zn
d110 (nm)	0.153	0.152	0.152
a (nm)	0.306	0.304	0.304
d003 (nm)	0.771	0.855	0.813
c(nm)	2.313	2.565	2.439
Interlayer-spacing (nm)	0.291	0.375	0.331

Table.4. BET data for samples

Sample	BET area (m^2/g)	Pores volume (ml/g)	Average pore size (nm)
LDHs	79.727	0.402	17.281
CLDHs	260.700	0.594	2.769

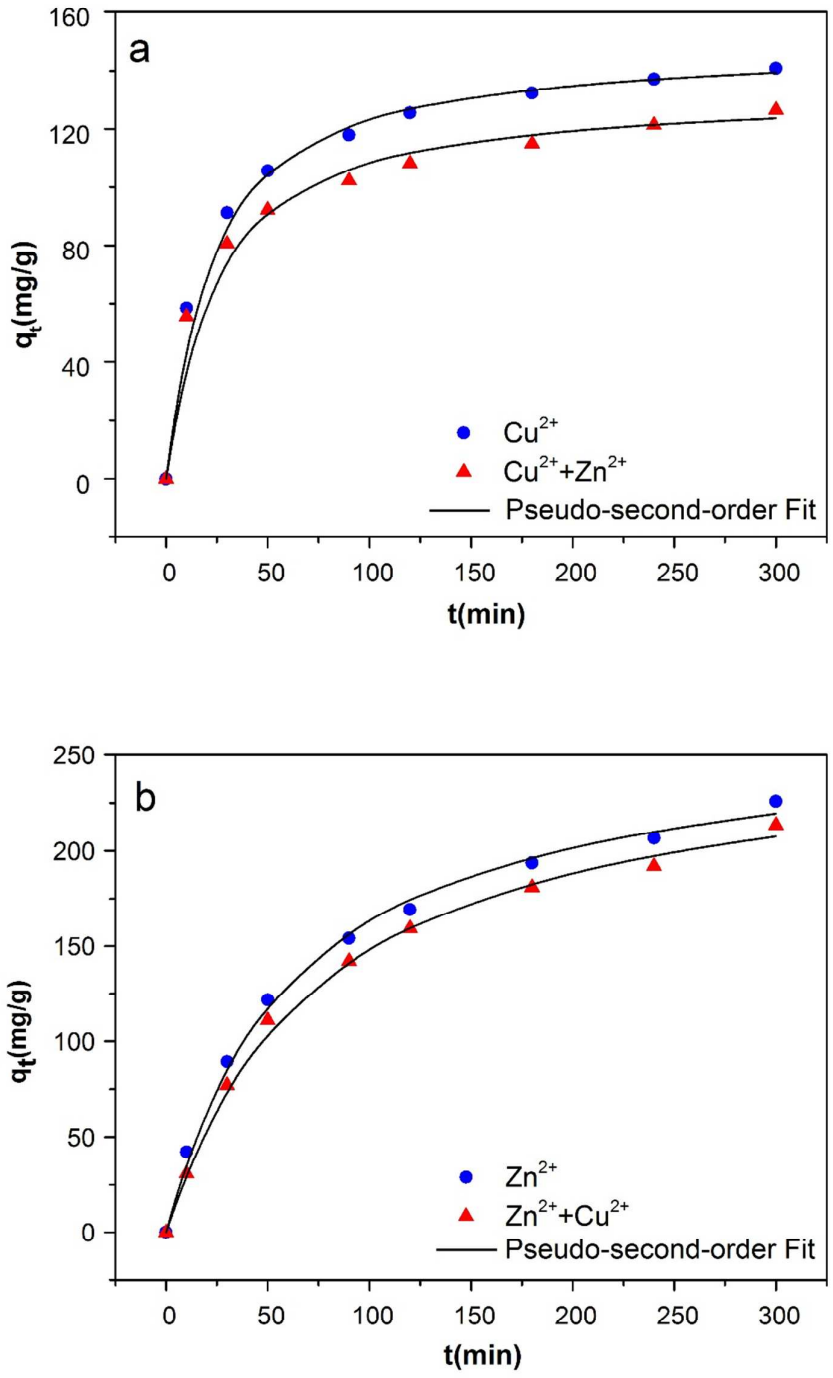

Fig.1. The pseudo-second-order models fit for (a) Cu^{2+} and (b) Zn^{2+} adsorption by CLDHs (a: $[Cu^{2+}]$=100mg·L^{-1}; $[Cu^{2+}+Zn^{2+}]$ =100 mg·L^{-1}+100mg·L^{-1}; b: $[Zn^{2+}]$=100mg·L^{-1}, $[Cu^{2+}+Zn^{2+}]$ =100 mg·L^{-1}+100mg·L^{-1})

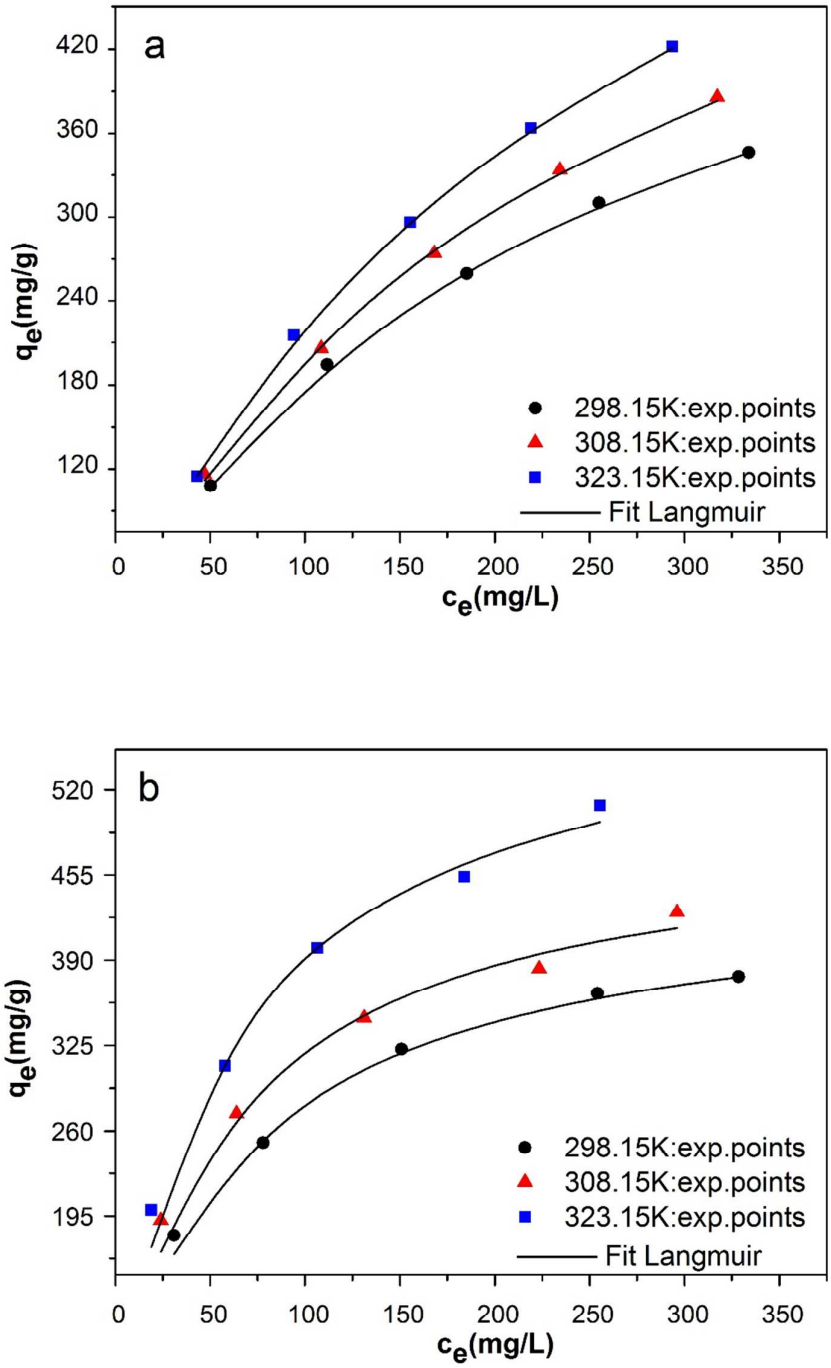

Fig.2. Model plots for the adsorption of (a) Cu^{2+} and (b) Zn^{2+} on CLDHs.

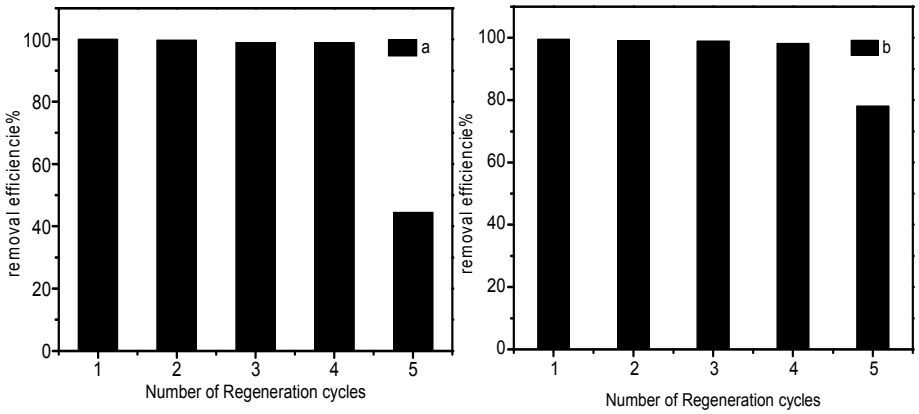

Fig.3. Removal efficiency of (a) Cu^{2+} and (b) Zn^{2+} in different cycles by using the CLDHs ($[Cu^{2+}]$=100mg·L^{-1}, $[Zn^{2+}]$=100mg·L^{-1}; T=308.15K, CLDHs= 0.3 g/100 mL).

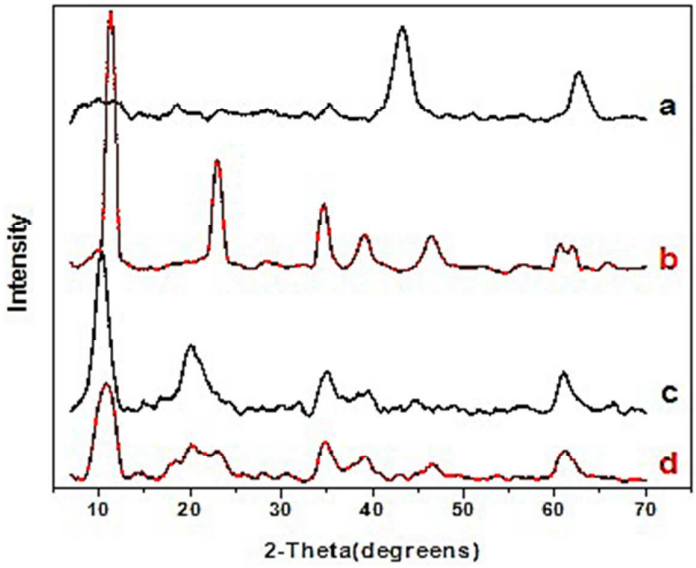

Fig.4. Powder XRD patterns for (a) CLDHs, (b) Mg_3Al-CO_3-LDHs, (c) CLDHs-Cu (after uptake of copper ion) and (d) CLDHs-Zn (after uptake of zinc ion).

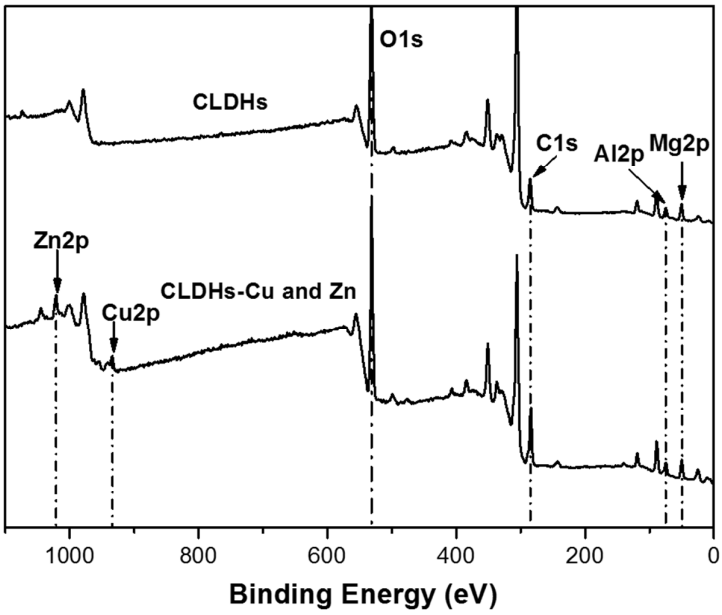

Fig.5. X-ray photoelectron spectra of pristine CLDHs and CLDHs-Cu and Zn.

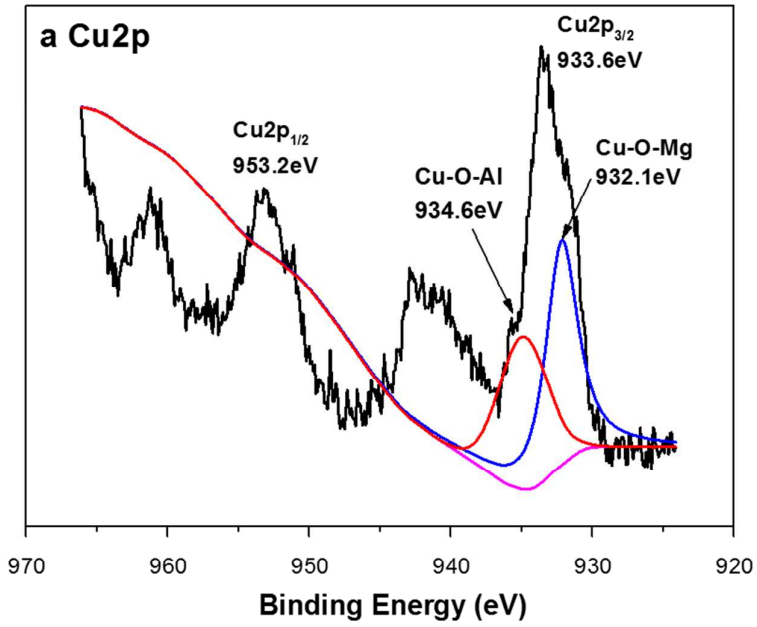

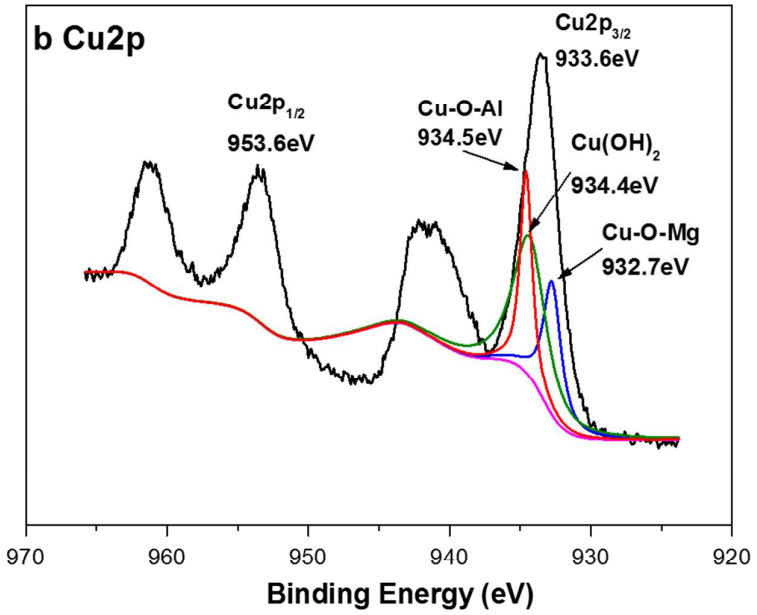

Fig.6. High-resolution XPS spectrum of (a) CLDHs-Cu-1 (adsorption of one cycle) and (b) CLDHs-Cu-2 (adsorption of five cycles until saturated)

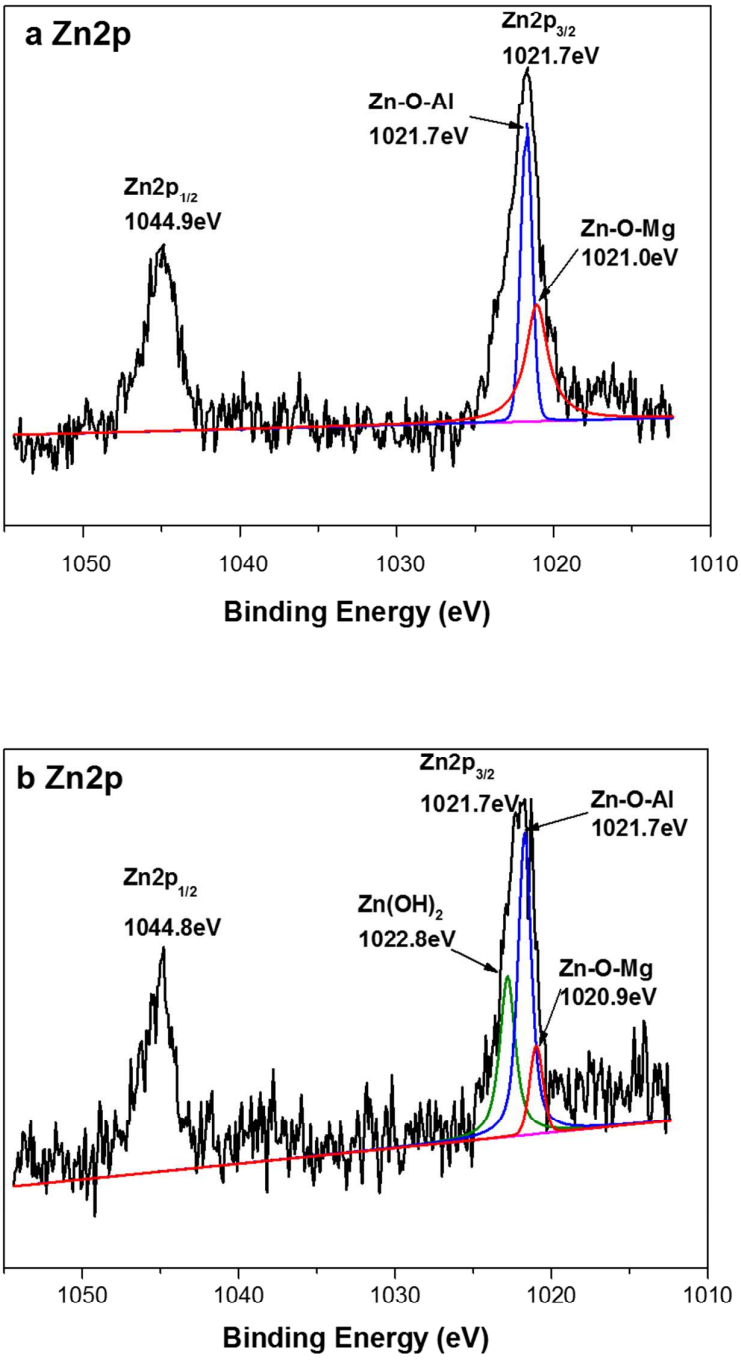

Fig.7. High-resolution XPS spectrum of (a) CLDHs-Zn-1 (adsorption of one cycle) and (b) CLDHs-Zn-2 (adsorption of five cycles until saturated)

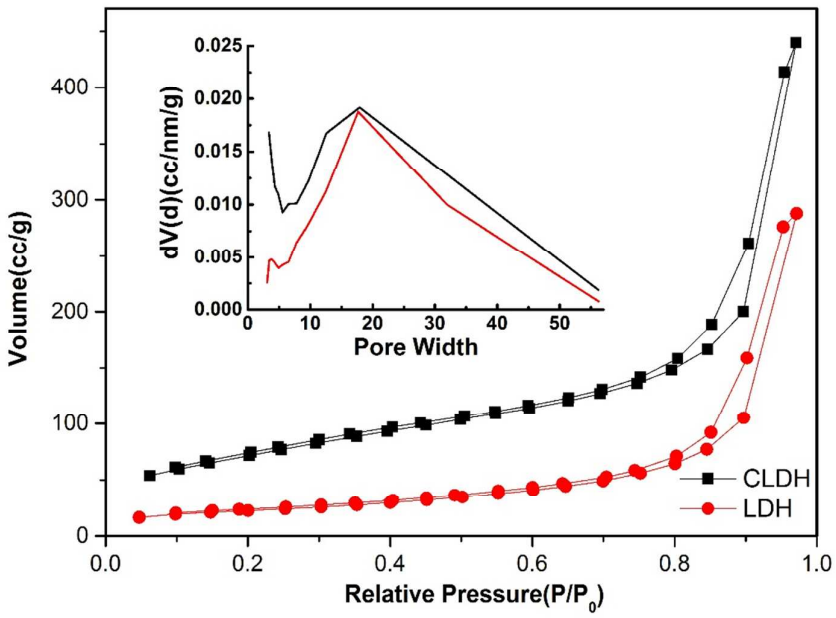

Fig.8. N_2 adsorption–desorption isotherms and pore size distribution (inset) of LDHs and CLDHs.

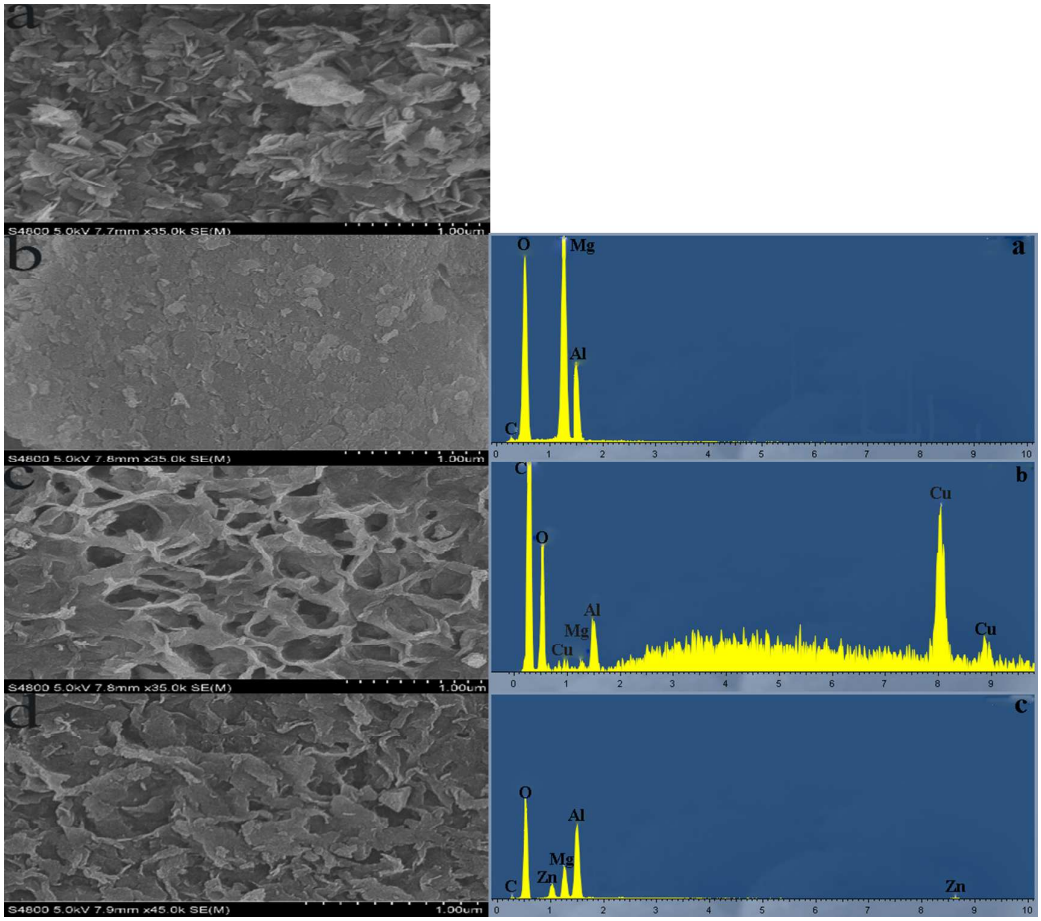

Fig.9. The SEM images of samples: (a) LDHs, (b) CLDHs, (c) CLDHs -Cu and (d) CLDHs-Zn. And the EDX of (a) CLDHs, (b) CLDHs-Cu and (c) CLDHs-Zn.